Paper presentation

“The Virgo O3 run and the impact of the environment”

Nicolas Arnaud, Theodoros Avgitas, Rosario DeRosa, Francesco Di Renzo, Irene Fiori, Kamiel Janssens, Alessandro Longo, Federico Paoletti, Paolo Ruggi, Maria C. Tringali
And
The Virgo Collaboration

https://arxiv.org/abs/2203.04014
(submitted to CQG)

KAGRA PEM meeting - May 19 2022

Introduction

- ## Focus of the paper:

  We used the 1-year long data sample to understand the behavior of the Virgo interferometer under different environmental conditions. Whenever possible, we identified relevant quantities which evidenced critical behaviors, and we described action plans to improve the detector performance.

- ## Topics:

  - Anthropogenic noise
  - Wind
  - Sea microseism
  - Earthquakes
  - Cosmic muons
  - Lightning's
  - Lock losses

1)

The Virgo site noise environment during O3

Virgo O3 environmental monitoring

Also:

- weather station
- external magnetometers
- cosmic muon detector

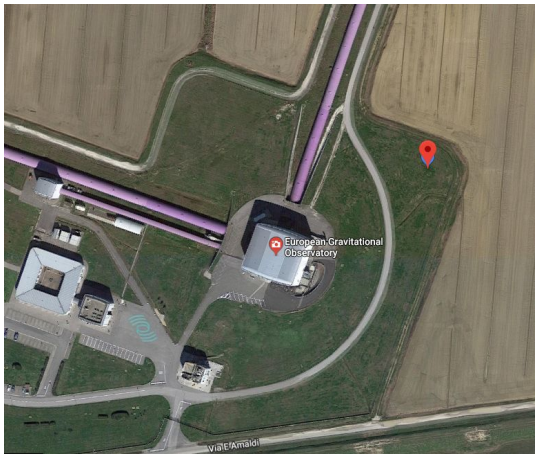

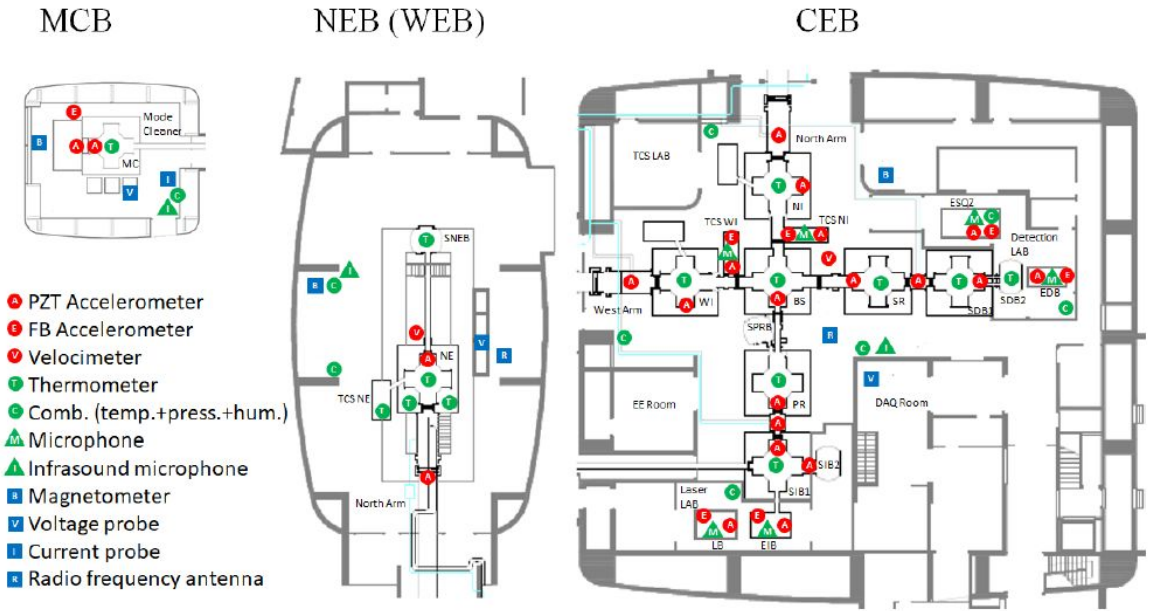

Noise spectra: seism and magnetic

Inside
External magnetometers
Quiet reference Sardegna - SosEnattos

SEISMIC - NEB Guralp 60s - NS
Percentiles - full O3 science mode dataset

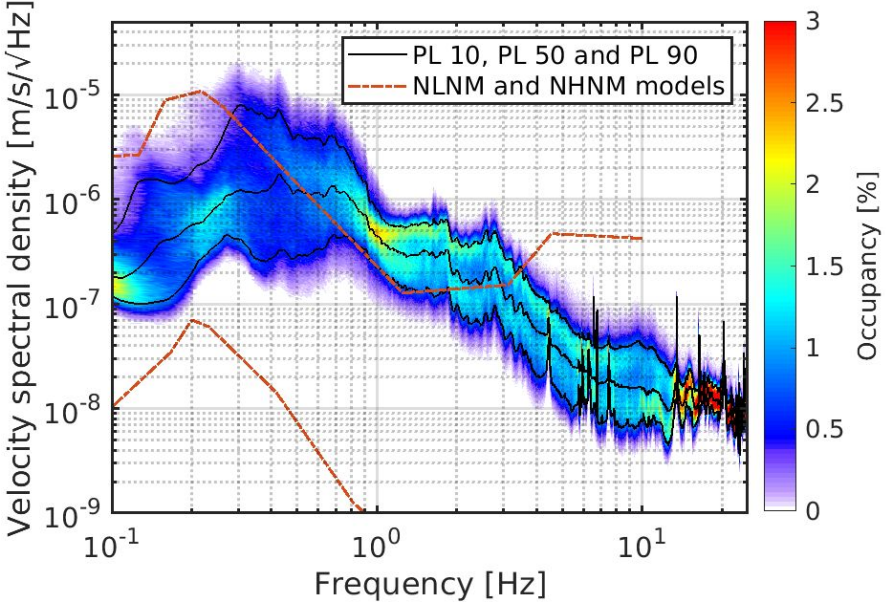

MAGNETIC - representative spectra

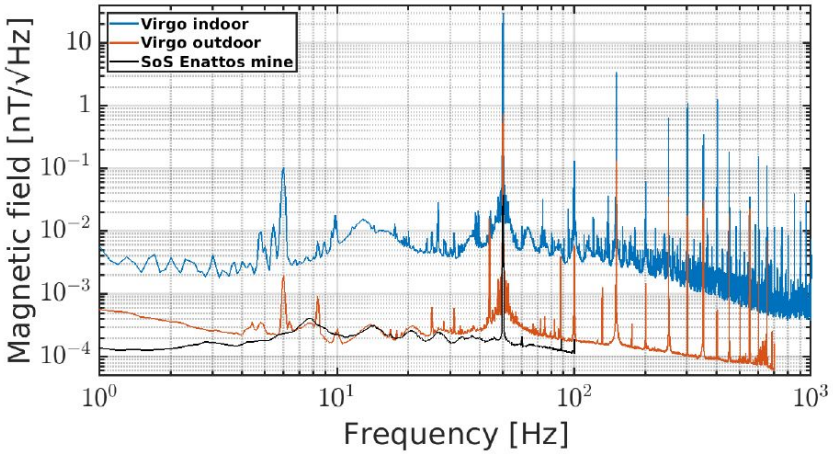

Figure 24: Amplitude spectral densities of indoor (blue curve) and outdoor (red curve) magnetometers at EGO and at Sos Enattos mine in Sardinia (black curve). The quiet Sos Enattos location shows evidence of Schumann resonances peaked at approximately 8, 14, 21, 27 and 33 Hz.

Noise statistics: micro-seism

RMS in [0.1,1 Hz] m/s

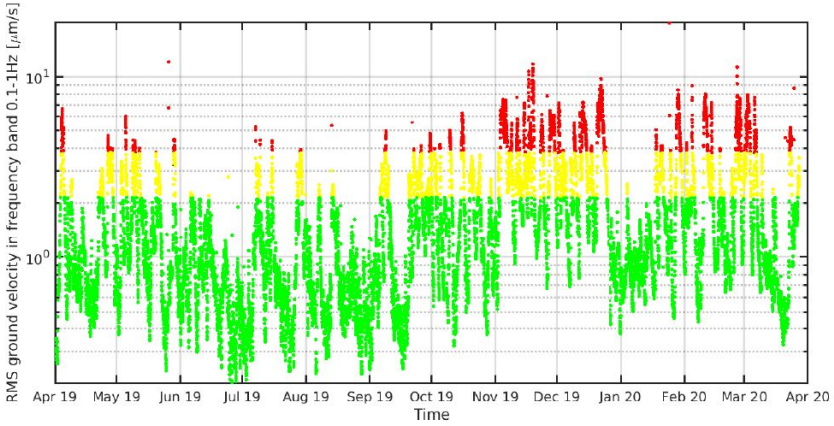

Figure 4: Evolution during O3 of seismic RMS in the 0.1 to 1 Hz frequency band. Data colored in yellow and red exceed the 75^{th} and 90^{th} percentile, respectively.

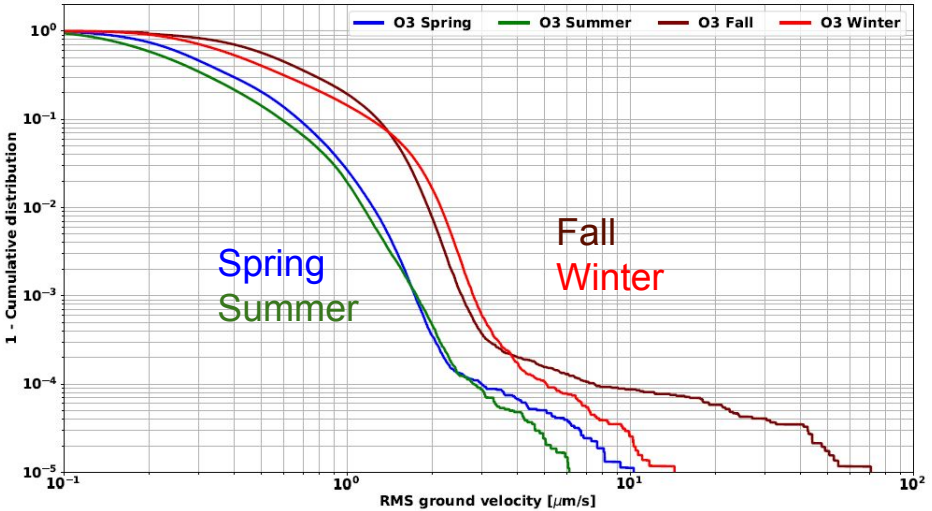

Figure 5: Cumulative distribution of microseism in the frequency band 0.1-1 Hz (dominated by sea activity), measured at EGO during each season in 2019-2020.

Noise variability - daily modulations: seism and magnetic

20% reduction during COVID lockdown (reduced traffic)

SEISMIC

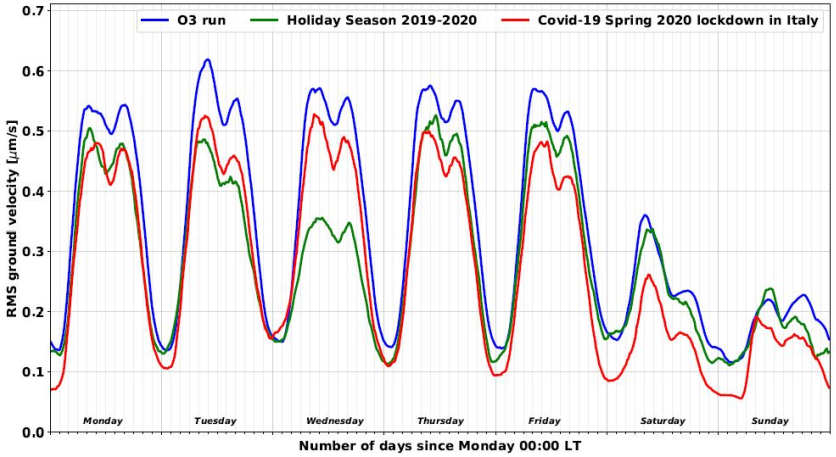

Figure 6: Average evolution on a weekly basis of the seismic anthropogenic noise (frequency band: 1-5 Hz) measured at EGO during different times in 2019-2020.

MAGNETIC

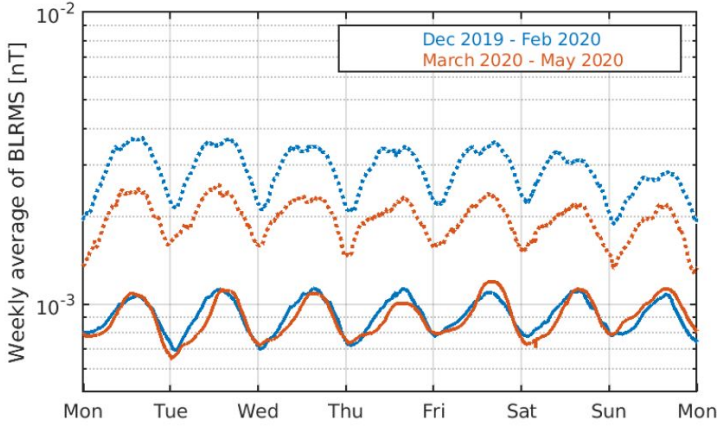

Figure 25: Weekly averaged magnetic field band-limited RMS values computed in two frequency bands: 1 to 6 Hz (dashed) and 18 to 24 Hz (solid). Magnetic field intensity is measured externally of Virgo experimental buildings, in the reference period between December 2019 and February 2020 (blue curves) and in the period between March 15 and May 15 (red curves) which corresponds to reduced anthropogenic activity within and outside of EGO because of the COVID-19 pandemics.

2)

Correlations between environmental noise and ITF

BNS range modulation

- BNS range changed often because of different reasons, besides environmental effects (e.g. changes in control accuracy)
- One way to averaging out occasional changes and evidence **persistent recurring effects** is looking at **BNS range fluctuations around its daily median level**. Here shown on a weekly timescale, averaged over O3.
- Daily modulation with deeps at midnights and reduced in weekends, **resembles anthropogenic noise from traffic**.

~1Mpc

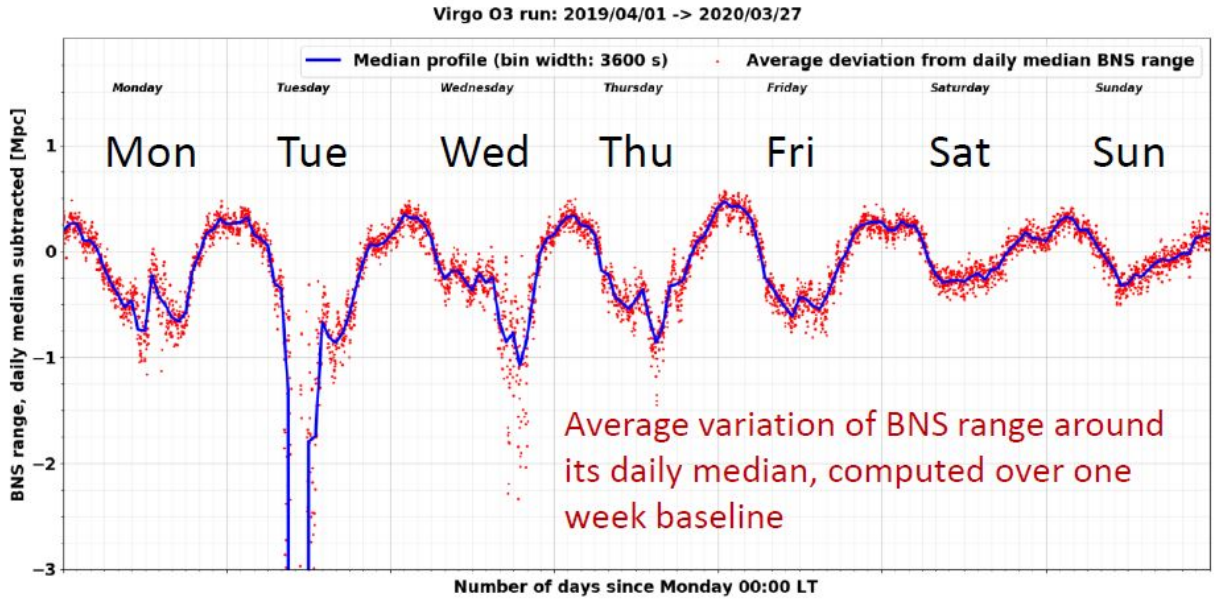

Impact of sea activity on sensitivity

- ***Hrec noise level was known to worsen during high microseism, particularly up to ≈ 40 Hz.***
- We show and quantify this correlation.
- A similar correlation is demonstrated between microseism and rate of short noise transients (glitches).

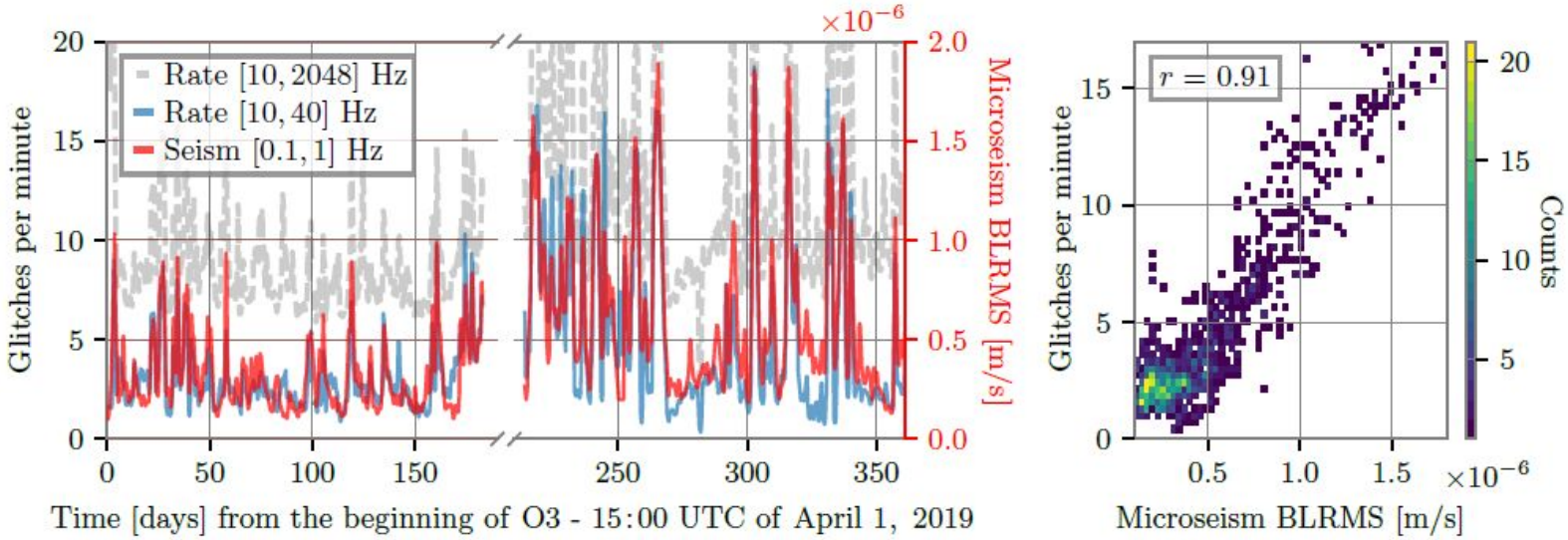

Microseism glitches are due to scattered light

- The non-stationary (glitch) noise during high-microseism conditions shows characteristic **scattered light arches**. Arch spacing (≈ 3s) matches microseism peak frequency.
- Most of the time, the noise arches are explained by the relative velocity of the **West End Suspended Bench** with respect to the TM.
- Typically the **SWEB moved much more than the West End Mirror** (Paolo Ruggi - VIR-0008A-21).
- An issue in SWEB suspension mechanics and control was identified and cured after O3.

Scattered light arches
well described by the motion of
suspended bench (SWEB) with
respect to WE test mass

$$f_{sc}(t) = \frac{2n|\dot{x}(t)|}{\lambda}$$

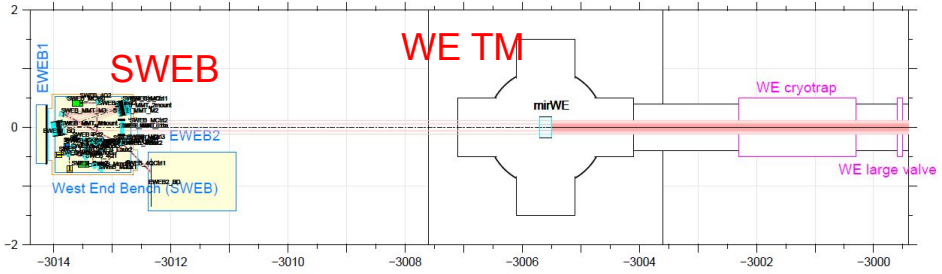

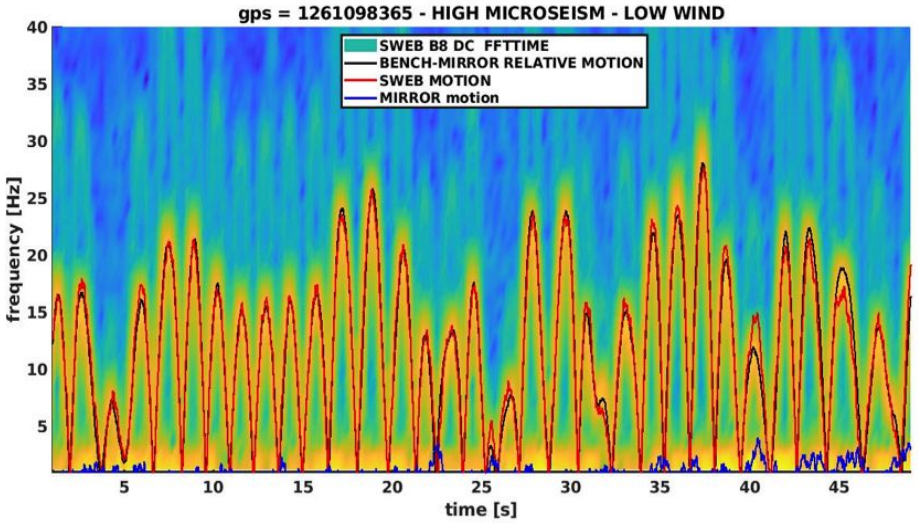

3)

Quantify robustness of ITF against the environment (bad-weather = wind and sea-activity)

Duty cycle during bad-weather

- ***During bad weather it was usually more difficult to keep the lock.***
- In bad weather, high wind and rough sea often are present together
- In order to disentangle which one (wind or sea) was more critical for ITF stability we relied on statistics.
- In the **selected low wind sample** (wind speed < 25 km/h) the duty cycle does not degrade significantly when microseism increases.
- We conclude that Virgo lock was **robust against microseism**

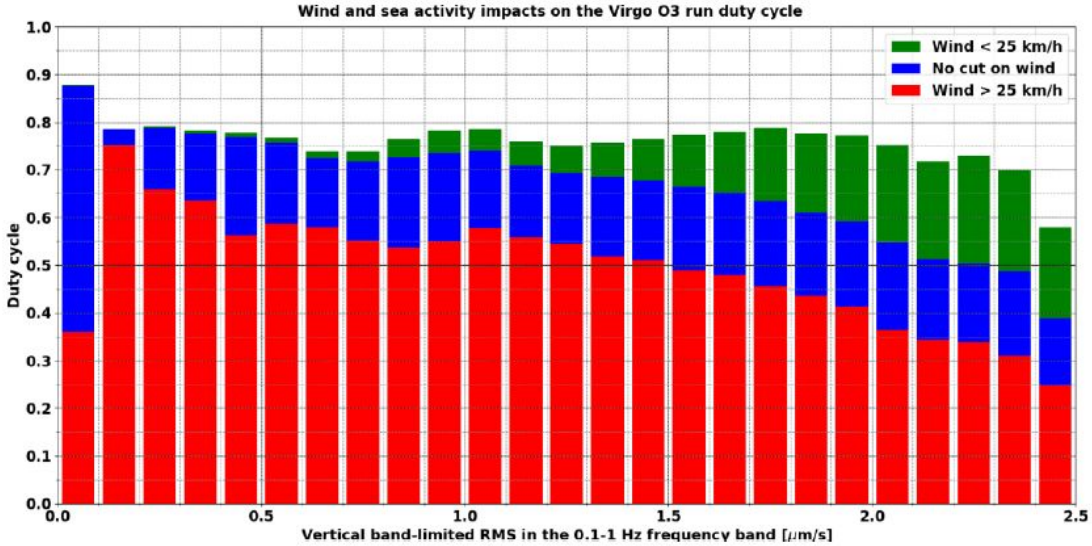

ITF duty cycle is measured as function of microseism level
(Duty cycle is the fraction of SCIENCE time in the given dataset)

Influence of wind on BNS range

- ***Virgo sensitivity during O3 was known to worsen during "bad weather" periods***, which often imply both high winds and intense sea activity.
- In order to quantify the impact of instantaneous wind speed on the sensitivity, the same quantity (BNS range deviation from daily average) is plotted as a function of average wind speed.
- **Sensitivity is unaffected until wind speeds of 20-25 km/h.**
- **For wind speeds of 50 km/h, 5 Mpc (10%) are lost.**

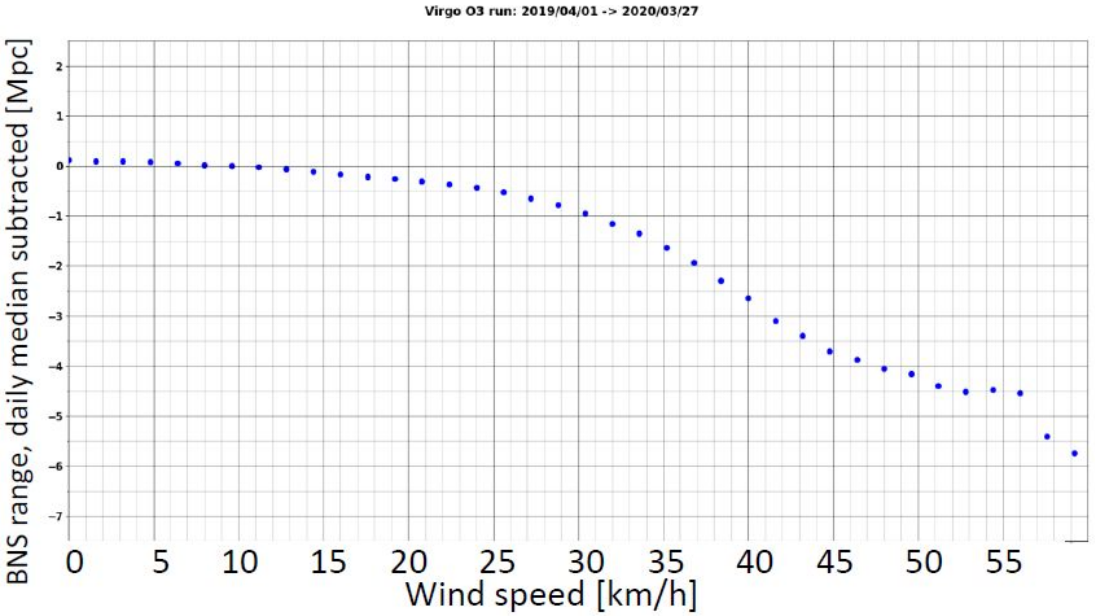

Average variation of BNS range from its daily median, as function of wind speed.

Wind is responsible for lock losses

- The higher the wind speed the larger the correction force (Volts) required to keep the lock. Close to 10 V the marionette actuators saturate and the lock is lost.
- → Lock-losses occur because of **saturation of the actuators** induced by **wind gusts**.
- **How to improve?** Upgrade the driving of INPUT marionettes equalizing them to the low noise setting implemented at the END marionettes. Then, we could use at the same time INPUT and END, gaining a factor of 2 in force, and a factor of sqrt(2) more noise (compliant with O4). We think that a factor of 2 more force will fix the problem of lock loss in any windy condition and many strong earthquakes.

Improve monitoring of wind gusts adding weather stations at end buildings.

Cumulative distribution of Max DARM correction versus wind speed

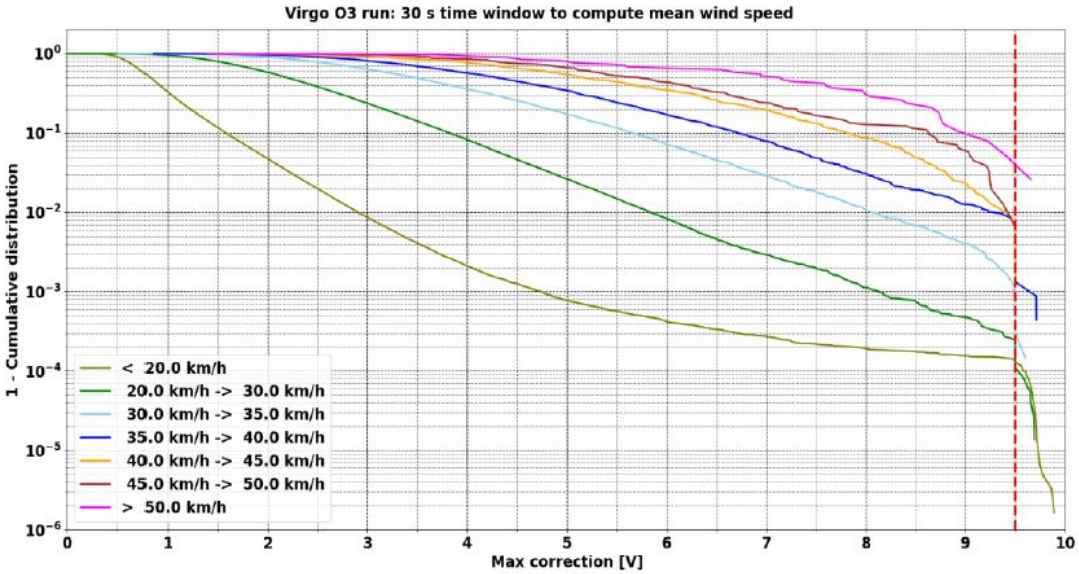

4)

Earthquakes, Lightnings and Cosmic muons

Earthquakes during O3

Early warning software *Seismon* (by LIGO) *was installed and operated during O3*

Seismon distributes EQ alerts (time, epicenter, magnitude) it receives from USGS and estimates P and S waves arrival time at Virgo.

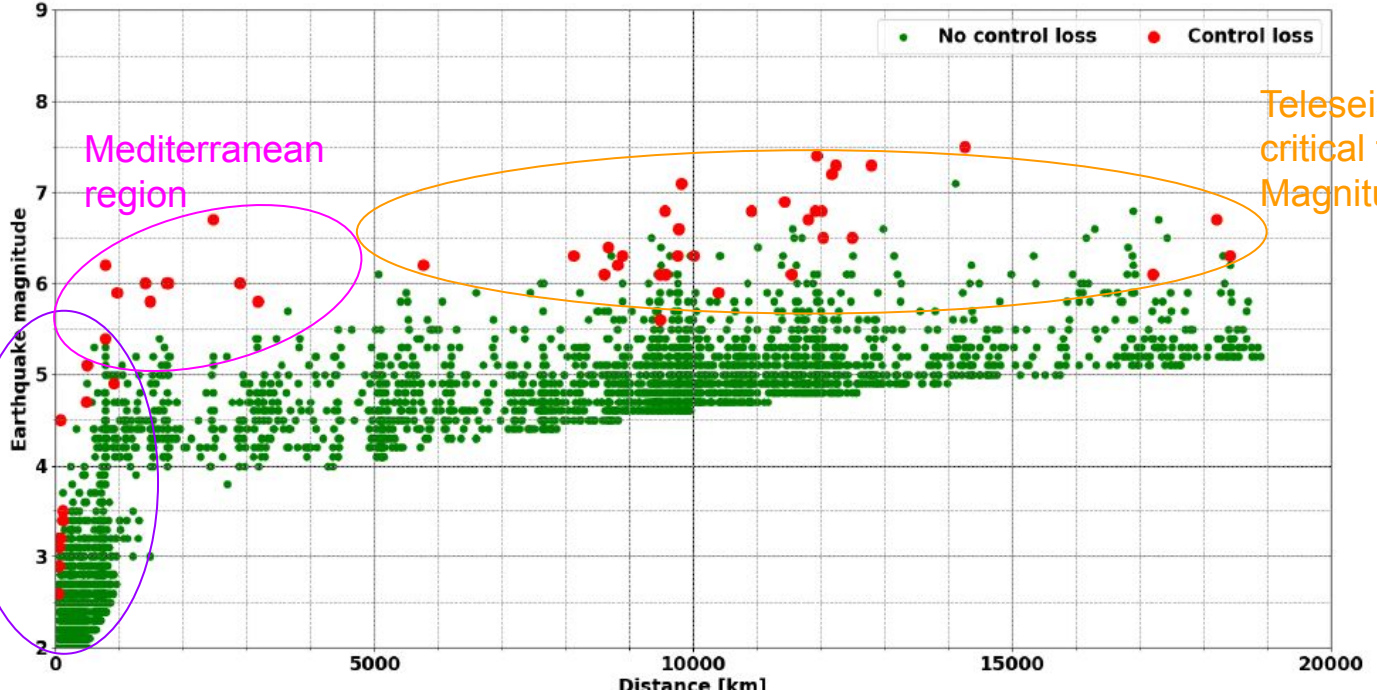

Italian EQ small but close

Mediterranean region

Teleseisms, critical threshold is Magnitude > 6

Earthquakes during O3

Seismon works well for distant earthquakes, not so much for closer EQ (Italy and mediterranean)

Plan is to improve by integrating in Seismon alerts from INGV (Italian institute of Geophysics) which has better coverage of this area.

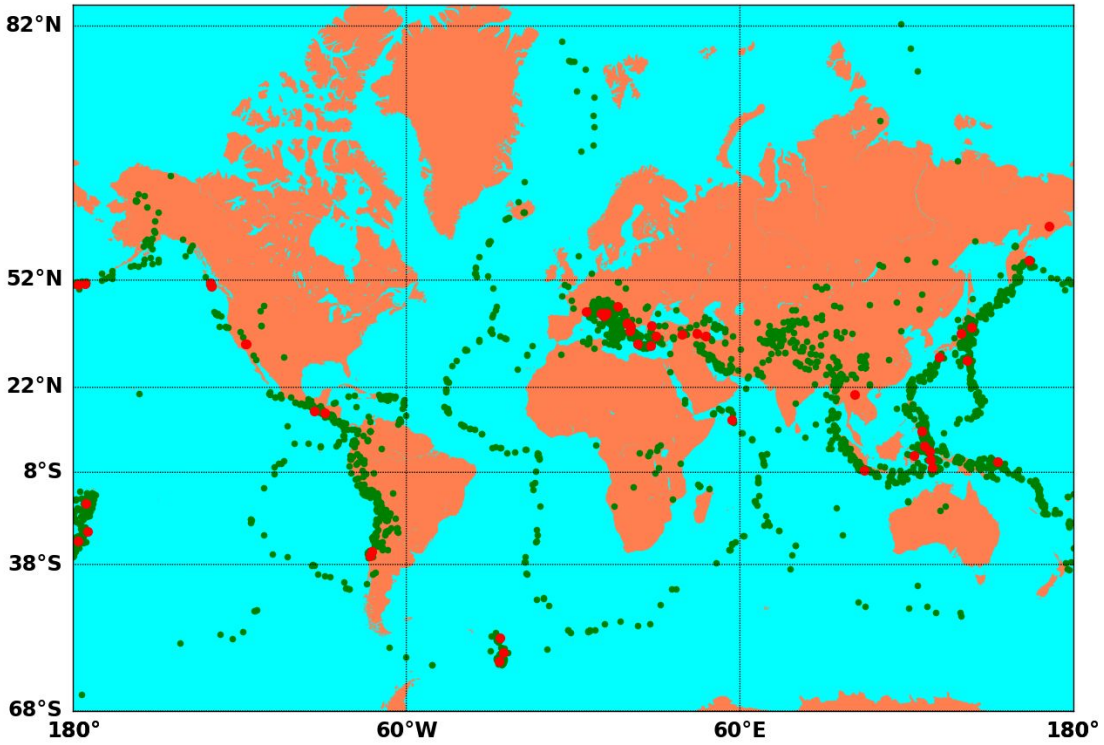

Impact of lightning strikes

- Magnetic pulse

  Excites suspension mechanical mode at 48Hz, likely acting on magnetic actuators

- Sonic pulse

  Triggers scattered light paths

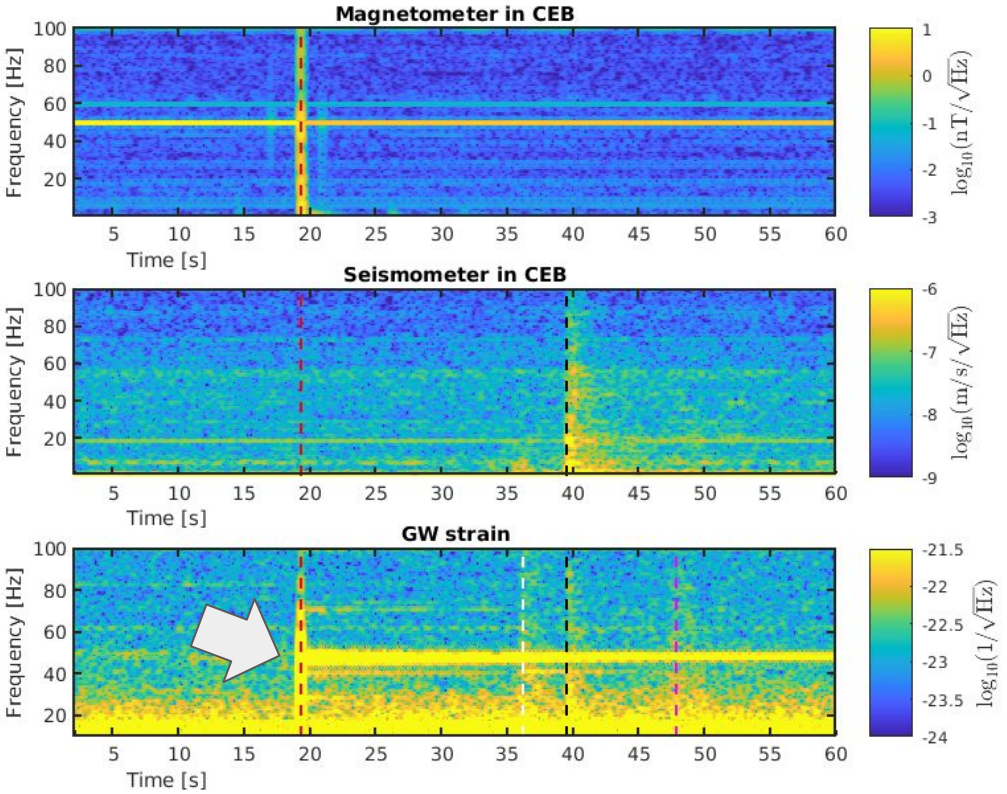

Cosmic muons

One telescope for cosmic muons was installed in CEB and operated for 14 days during O3

Seven GW alerts occurred during this period (4 public). Found no statistical evidence of an excess of muons in correspondence of these events.

The muon rate and the glitch rate are both correlated with the environment (mainly atmospheric pressure) but that there is no causation identified between the two.

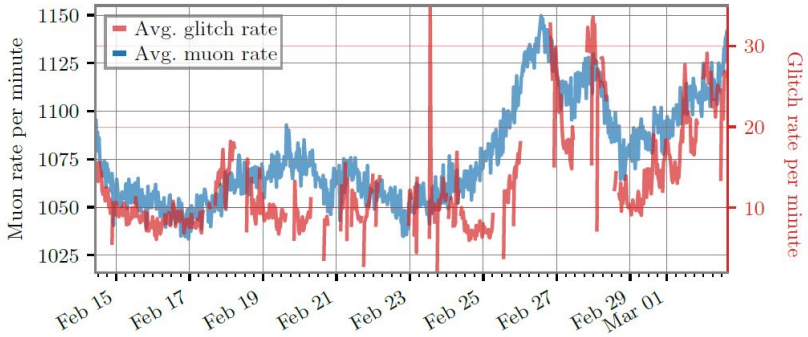

Muon rate

Atmospheric pressure

Temperature

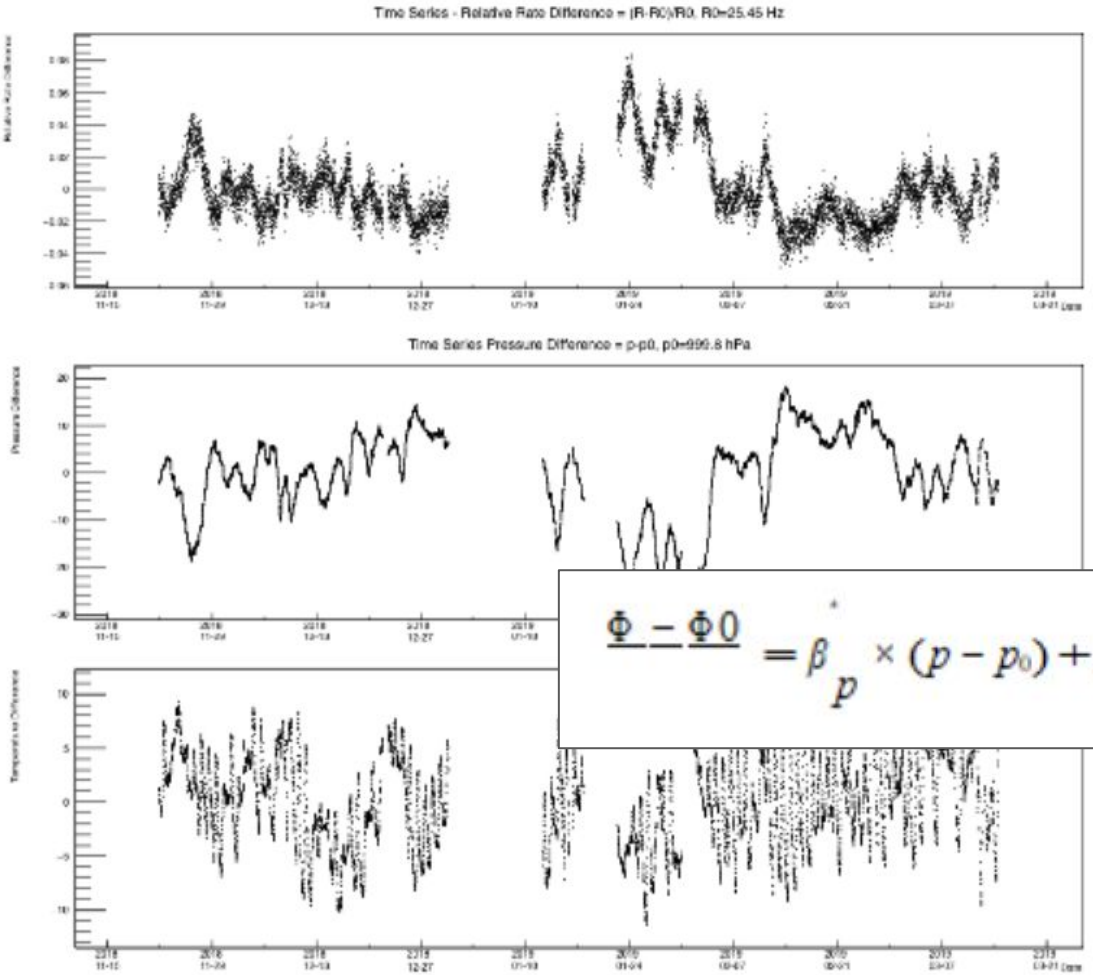

$$\frac{\Phi - \Phi 0}{} = \beta_{p}^{*} \times (p - p_0) + \beta_{T}^{*} \times (T - T_0),$$

Figure 2: Data time series in time intervals of 1000 seconds. (a) Muon rate is calculated as the mean value at time t0 +/- 500 s. (b) Pressure and (c) Temperature both measured at ground level. The quantities plotted here are explained in the top of each diagram.